# BEAM DIAGNOSTICS AT THE JINR PHASOTRON

V.V.Kolga, L.M.Onishchenko, M.F.Shabashov, N.G.Shakun, A.L.Shishkin

Joint Institute for Nuclear Research, Dubna

At the JINR phasotron [1] the protons are accelerated up to 660 MeV. Such parameters of the beam as its intensity, dimensions, axial position, beam losses during acceleration and extraction should be measured for the optimization of the acceleration process.

In the central region of the accelerator up to the radius of 70 cm the beam current probes are used. The dependences of the beam intensity measured with such a probes on the radius and on the rotation speed of the rotating capacitor are shown in Fig. 1.

On the larges radii the pick-up electrodes are used. Six pairs of the pick-ups are placed in the region from 247 cm to 272 cm with the same distance of 5 cm. The radial width "2b" of the pick-ups is 4.5 cm, their azimuthal size "2$\alpha$" is 4° and the axial aperture "2a" is 10 cm.

The pick-ups are used for the prompt measurement of the beam axial position, its phase width and time duration, average intensity and for estimation of the beam radial size.

The axial beam position "Z" with regard to the median plane is given by

$$z = a \cdot \frac{U_u - U_\ell}{U_u + U_\ell} \qquad (1)$$

where $U_u$, $U_\ell$ are the signals induced by the beam in the upper and lower pick-ups, respectively.

For measuring the beam position the signals from the upper and lower pick-ups are purified from the induced parasitic signal with the harmonic analysis.

The accuracy of this measurement taking into account the vertical size of the beam is about ±1.5 mm. Each pick-up is loaded by the cable with the impedance $\rho$=50 Ohm, therefore the pick-up signal is proportional to the charge change velocity under the pick-up and the average beam intensity I can be calculated by the double integration over the azimuth of the pick-up signal [2]

$$I = \frac{F}{2b \cdot \rho \cdot f \cdot 2\alpha} \cdot \frac{a^2 - z^2}{2a} \cdot \int_0^{2\pi} d\varepsilon \int_\delta^{\varepsilon} \left[ U_u(\varphi) + U_\ell(\varphi) \right] \cdot d\varphi \,, \qquad (2)$$

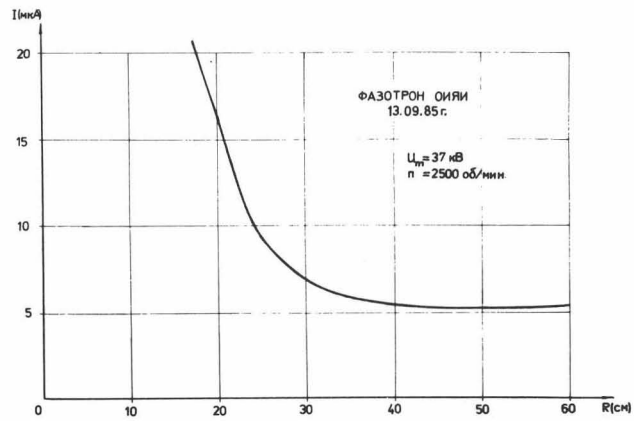


a) along radius

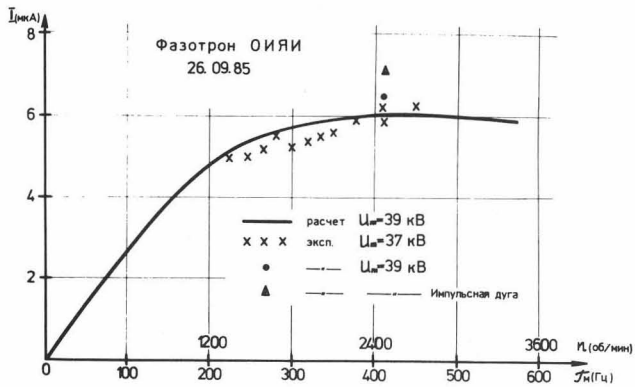


b) along rotating capacitor rate

Fig. 1. Beam intensity from the current probe.

where $f$ is the orbit frequency of the beam on the pick-up radius, $F$ is the modulation rate.

Practically, pick-up signals are used for the relative measurements of the beam intensity.

The radial size of the beam is determined using the time of the beam passing under the pick-up by comparison of the pick-up macrosignal $u(t)$ (Fig. 2*) with the pick-up sensitivity curve to the zero radial size charge, which is given by

$$K(x)=K_0^{-1}\left\{\frac{x+b}{[a^2+(x+b)^2]^{1/2}}-\frac{x-b}{[a^2+(x-b)^2]^{1/2}}\right\},$$

$$K_0=2\cdot(a^2+b^2)^{-1/2}, \qquad (3)$$

where $x=r-R$ is the beam radial position with regard to the centre of the pick-up.

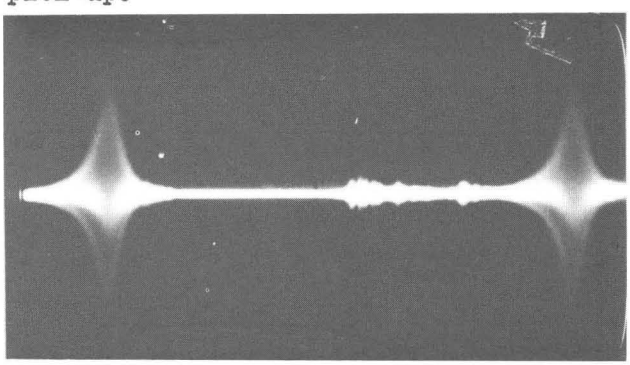

a) accelerated beam

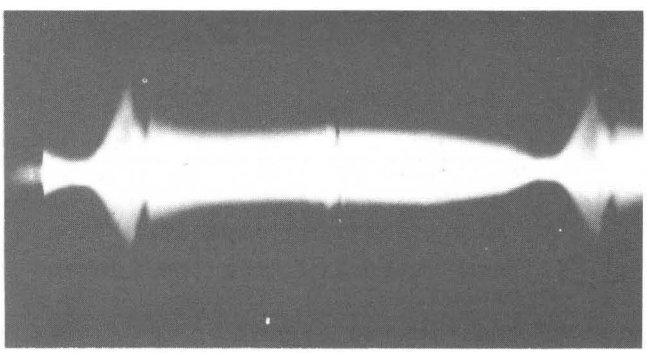

b) stretched beam

Fig. 2. Signal from the pick-up $u(t)$ at 267 cm (time scale 0.5 ms/cm).

* For comparison the signal from the pick-up placed on the radius 272 cm is shown, when the stretched beam is passing under the pick-up with a radial velocity 100 times lower than the normal one.

Using the known velocity of the beam-radial displacement (see below), $u(t)$ can be transformed to $u(x)$ and then the beam radial size is defined as $\Delta X=\Delta U(x)-\Delta K(x)$, where $\Delta U(x)$ and $\Delta K(x)$ are the fwhm of the respective curve (Fig. 3).

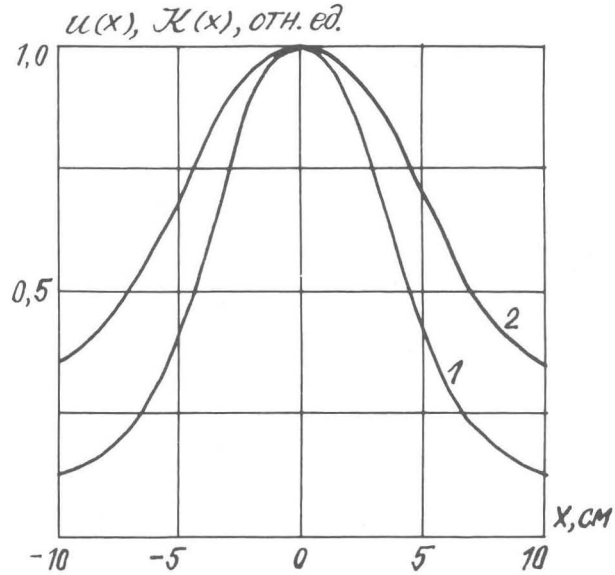


Fig. 3. Curve: 1 - calculated pick-up signal $K(x)$ for the beam of zero radial width; 2 - real pick-up signal $u(x)$.

For the extracted beam current of 1.5 $\mu$A the beam radial size is 50±10 mm.

This method though not highly accurate is convenient for the prompt estimation when the acceleration conditions are changed.

Another device widely used in the beam diagnostics is the secondary emission monitor (SEM).

Thus, for measurement of the extracted beam parameters two SEMs are installed in the vacuum chamber just before the extraction window. Each SEM consists of a thin aluminum foil in the beam path and an integral (for the intensity measurement) and differential (for the profile measurement) collector.

In Fig. 4 the beam vertical and horizontal profiles are shown. The description of this SEM construction is given in 3), while its circuit diagram is in 2).

For accelerated beam measurement a SEM displaced along the radius is used. It is schematically shown in Fig. 5.

The foils which are used in the SEM have the radial width "d" of 1÷3 mm and the thickness along the beam path of about 2 mg/cm$^2$. Because of the limited thermal stability of the foil the special ion source mode is used in these measurements with the duty cycle of 1:10.

The SEM operates in two different modes: a) with the integration time con-

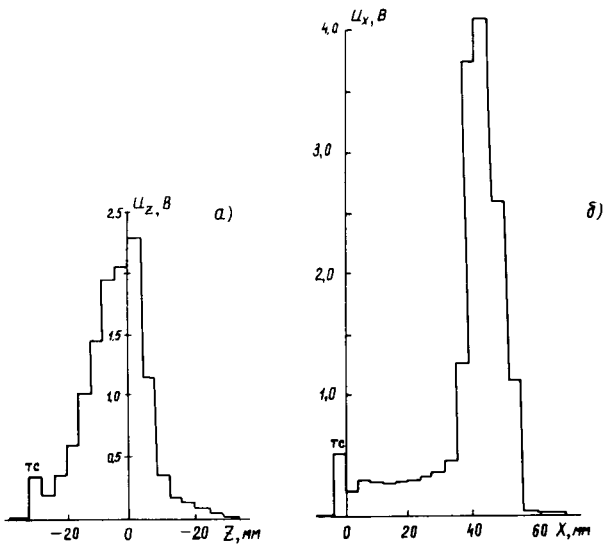


Fig. 4. Extracted beam charge distribution: a) axial, b) horizontal.

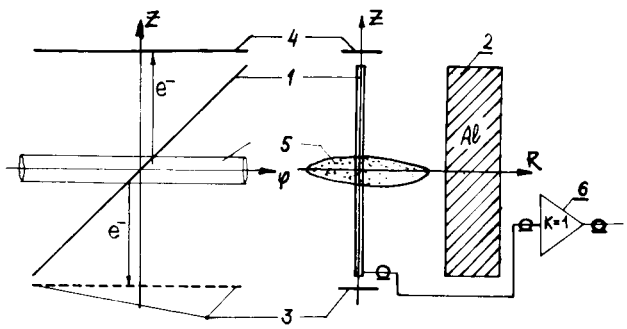


Fig. 5. Schematic view of SEM.

stant of 100 ms; b) with the integration time constant of 1 μs.

The first mode is used for the beam intensity and for the beam losses measurements during the acceleration process. In this case the SEM signal

$$U = I \cdot n \cdot \gamma \cdot R_{in} \quad , \qquad (4)$$

where "I" is the beam average current; "n" is the recurrence of the proton passing through the foil; $\gamma$ is the secondary emission factor, which is proportional to the stopping power dE/dx and depends on the proton energy; $R_{in}$ is the input impedance of an amplifier.

It is shown in [3], that the recurrence in the JINR phasotron does not depend on the radial oscillations amplitudes and is equal to

$$n = d \cdot f \cdot \left(dR/dt\right)^{-1} \quad , \qquad (5)$$

where $dR/dt$ is the radial speed of the beam. Between the foil and the collectors for collection of the secondary electrons the voltage of 100 V is applied, the signal from the foil comes to the input of the amplifier, placed just in the probe head.

The signal treatment eliminates from it the parasitic voltage induced by the accelerating field. The value of the parasitic voltage depend on the SEM radius and is equal to zero on radii longer than 150 cm.

The second mode (with a small time constant) is used to measure the radial speed of the beam displacement and its radial size.

Evidently, the beam-foil interaction time depends on the beam radial size $\Delta X$ and its radial displacement speed $dR/dt$. Fig. 6 shows the speed $dR/dt$ measured with the SEM and (solid line) calculated with the known dependences of the magnetic field, the accelerating voltage and its frequency on radius.

An irregularity, which is seen on the curve is explained by the magnetic field variation. It is important to note that the measured values of $dR/dt$ do not depend on the accelerating voltage, which is essential for what follows.

The radial size of the beam is formed by the amplitudes of the synchrotron and betatron oscillations. As for the betatron oscillations, their amplitudes only depend on the accelerating voltage value at the capture, while the maximum

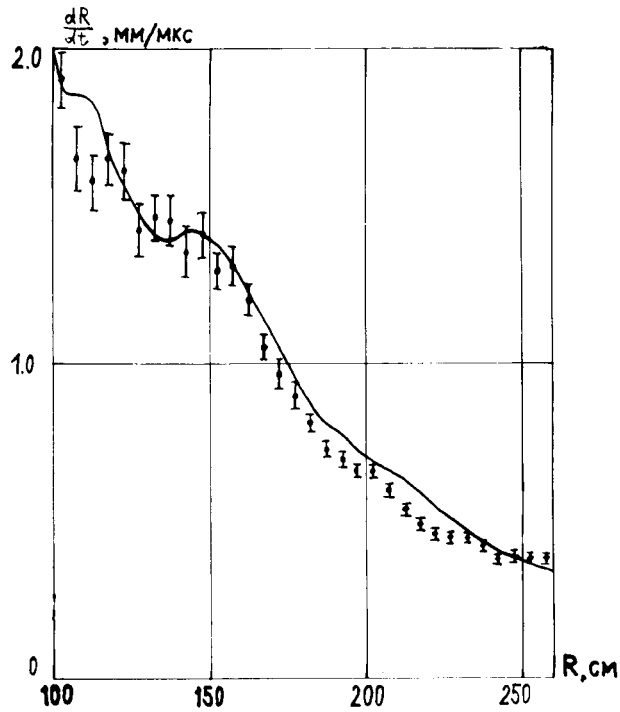


Fig. 6. dR/dt along the radius; points - measured values; solid line - calculation.

synchrotron amplitude is determined by the separatrix size in the acceleration process.

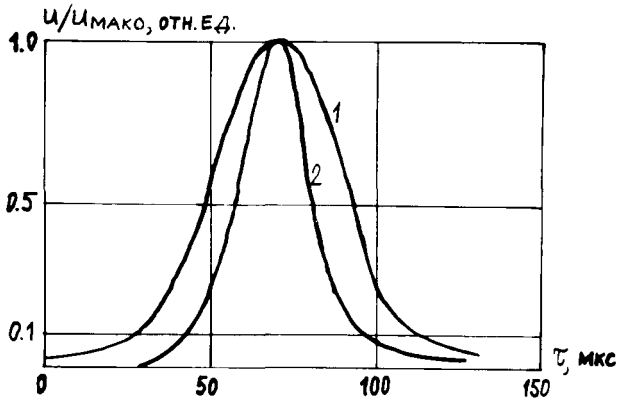


Fig. 7. SEM normalized signals at R=245 cm: 1 - with nominal value of accelerating voltage; 2 - with decreased accelerating voltage.

To estimate the radial betatron amplitude one decreases the accelerating voltage in some section of the acceleration cycle until the SEM signal is still reliable and after that the radial size of the beam passed through this section is measured. In Fig. 7 the normalized SEM signals are shown for different values of the accelerating voltage $U_d$. The measured values of the beam radial width are listed in Table 1 for different (0.1 and 0.5) levels of the SEM signal amplitudes.

The extracted beam intensity in this measurement was 1 μA, the SEM was placed on the R=245 cm, the accelerating voltage was changed in the frequency region 15.5 ÷ 15.0 MHz, which corresponds the radius region 235 ÷ 260 cm.

The values given in Table 1 strongly depend on the acceleration mode particularly on the beam current. The results of the measurements for two values of the extracted beam current are listed in Table 2 for $U_d = 0.56 \cdot U_{d\,nom}$ and for the radius of 245 cm.

The values in Table 2 are interpreted as the maximum amplitudes of the betatron oscillations. Thus, for the extracted beam current of 2 μA the maximum amplitude of these oscillations is 21±2 mm while for 1 μA it is 12.5±2 mm.

The simultaneous measurements with SEM and pick-ups showed that for the radii more than 245 cm the foil doesn't produce visible distortions in the beam charge distribution.

The SEM mode with the high time constant is also used to measure the axial size of the beam and its axial position with the help of the differential collectors (Figs 8, 9). In this case the axial distribution was reconstructed with allowance for dispersion of particles from multiple passing through the foil [3].

The same SEM mode is used for the investigation of the accelerated beam losses. It is found that the particles lost due to the phase losses are localized at the losses radius while their number decreases in time due to dispersion in the foil with the time constant about 20 ms. Thus, the multiplicity of the lost particles passing through the foil increases and, as seen from (4), the SEM signal in this case will grow. The dependence of the SEM signals on the radius for this case is shown in Fig. 10; curve 1 corresponds to the normal acceleration process with the extracted beam current of 2 μA, curve 2 corresponds to the regime with the phase beam losses in the 180÷200 cm radial zone due to accelerat-

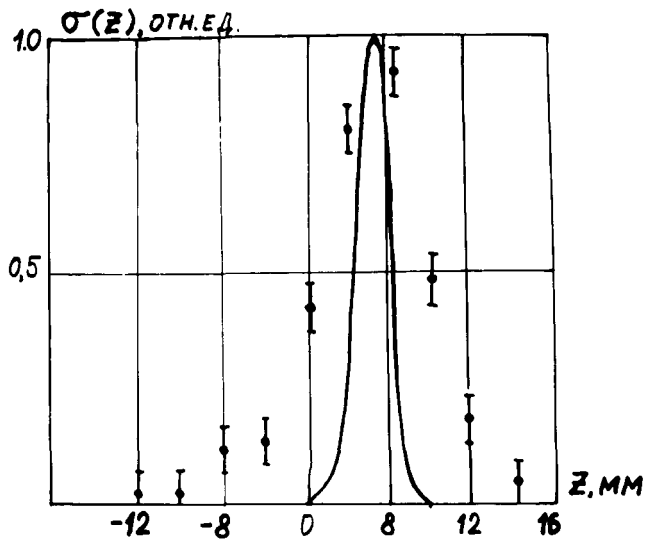


Fig. 8. Axial distribution of the beam charge at R=245 cm (solid line). Points - SEM signal values.

Table 1.

| $U_d/U_{dnom}$ | 1.0 | 0.91 | 0.78 | 0.74 | 0.69 | 0.61 | 0.56 |
|---|---|---|---|---|---|---|---|
| $\Delta X_{0.1}$, mm | 43 | 42 | 37 | 35 | 30 | 26 | 25 |
| $\Delta X_{0.5}$, mm | 22 | 21 | 18 | 16 | 14.5 | 13.5 | 12 |

Table 2.

| I, μA | 1.0 | 2.0 |
|---|---|---|
| $0.5\Delta X_{0.1}$, mm | 12.5±2 | 21±2 |
| $0.5\Delta X_{0.5}$, mm | 6±2 | 10±2 |

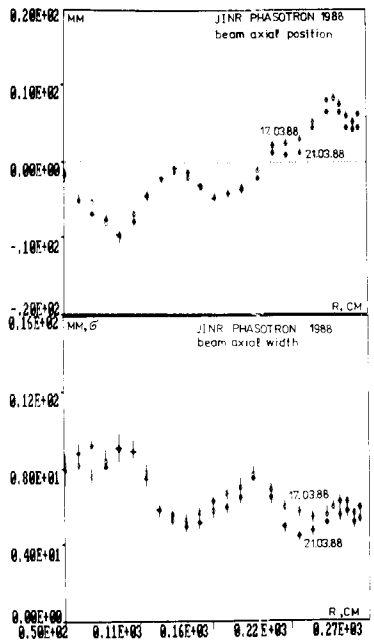


Fig. 9. Axial position (a) and size (b) of the beam along the radius.

ing voltage decreasing in this zone.

The knowledge of the multiplicity of the beam passing through the foil allows the beam extraction efficiency to be determined. For this purpose the induced activities of $^{24}Na$ in the aluminum foils are compared, one foil being exposed to the extracted beam and the other to the preextracted beam. The extraction efficiency determined in this way is 52 ÷ 56%.

So the devices which are used at the JINR phasotron for the beam diagnostics allowed the process of the beam acceleration and extraction to be investigated quite thoroughly.

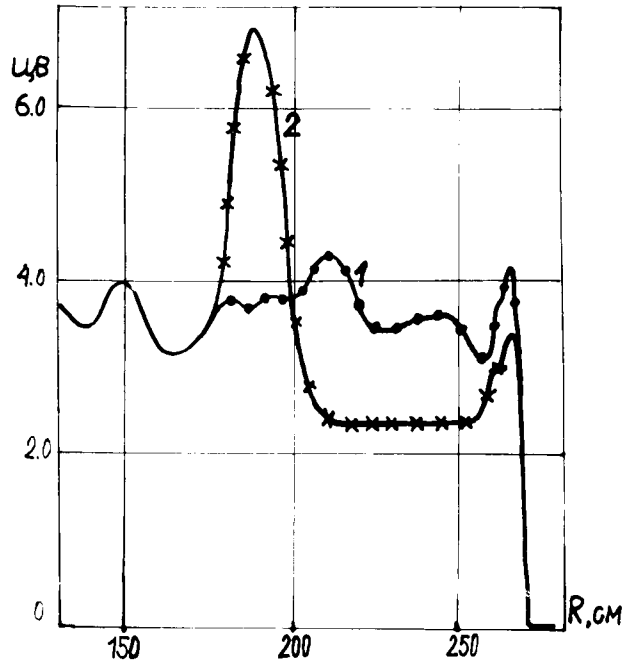


Fig. 10. Beam intensity along the radius (detected by SEM): 1 - with nominal accelerating voltage; 2 - with 1.5 times decreased accelerating voltage within 180 ÷ 200 cm.

References

1) A.T.Vasilenko, et al. Proceedings of the 10th All-Union Meeting on the Accelerators, v. II, p. 228, Dubna, 1987.

2) Ju.N.Denisov, et al. ibid. v. 1, p. 56.

3) A.A.Belyaev, et al. JINR 13-88-575, Dubna, 1988.